

THE NATIVE T-TYPE CALCIUM CURRENT IN RELAY NEURONS OF THE PRIMATE THALAMUS

G. M. ALEXANDER,^a W. B. CARDEN,^b J. MU,^b
N. C. KURUKULASURIYA,^b B. A. McCOOL,^c
B. K. NORDSKOG,^b D. P. FRIEDMAN,^c J. B. DAUNAIS,^c
K. A. GRANT^c AND D. W. GODWIN^{a,b,*}

^aThe Neuroscience Program, Wake Forest University School of Medicine, Medical Center Boulevard, Winston-Salem, NC 27157, USA

^bDepartment of Neurobiology and Anatomy, Wake Forest University School of Medicine, Medical Center Boulevard, Winston-Salem, NC 27157, USA

^cDepartment of Physiology and Pharmacology, Wake Forest University School of Medicine, Medical Center Boulevard, Winston-Salem, NC 27157, USA

Abstract—The generation of thalamic bursts depends upon calcium currents that flow through transiently open (T)-type calcium channels. In this study, we characterized the native T-type calcium current underlying thalamic burst responses in the macaque monkey. Current clamp recordings from lateral geniculate nucleus (LGN) slices showed characteristic burst responses when relay cells were depolarized from relatively hyperpolarized membrane potentials. These bursts could also be elicited by stimulation of excitatory synaptic inputs to LGN cells. Under voltage clamp conditions, the inactivation kinetics of native currents recorded from primate LGN neurons showed consistency with T-type currents recorded in other mammals and in expression systems. Real-time reverse transcriptase PCR performed on RNA isolated from the LGN (including tissues isolated from magnocellular and parvocellular laminae) detected voltage-dependent calcium channel (Ca_v) 3.1, Ca_v 3.2, and Ca_v 3.3 channel transcripts. Ca_v 3.1 occurred at relatively higher expression than other isoforms, consistent with *in situ* hybridization studies in rats, indicating that the molecular basis for burst firing in thalamocortical systems is an important conserved property of primate physiology. Since thalamic bursts have been observed during visual processing as well as in a number of CNS disorders, studies of the expression and modulation of these currents at multiple levels are critical for understanding their role in vision and for the discovery of new treatments for disruptions of thalamic rhythms. © 2006 IBRO. Published by Elsevier Ltd. All rights reserved.

Key words: lateral geniculate nucleus, burst, EPSP, monkey, cynomolgus macaque, epilepsy.

*Correspondence to: D. W. Godwin, Department of Neurobiology and Anatomy, Wake Forest University School of Medicine, Medical Center Boulevard Winston-Salem, NC 27157, USA. Tel: +1-336-716-9437; fax: +1-336-716-4534.

E-mail address: dgodwin@wfubmc.edu (D. W. Godwin).

Abbreviations: ACSF, artificial cerebrospinal fluid; Ca_v, voltage-dependent calcium channel; cDNA, complementary DNA; C_T, threshold cycle; EPSP, excitatory postsynaptic potential; IPSP, inhibitory postsynaptic potential; *k*, slope coefficient; LGN, lateral geniculate nucleus; NMDA, *N*-methyl-D-aspartate; RT-PCR, reverse transcriptase PCR; T-type, transiently open-type; TTX, tetrodotoxin; V_{1/2}, half-maximal inactivation.

0306-4522/06/\$30.00+0.00 © 2006 IBRO. Published by Elsevier Ltd. All rights reserved.
doi:10.1016/j.neuroscience.2006.03.042

The past decade has seen an explosion of knowledge of the molecular properties and functional roles of calcium channels (for review, see Perez-Reyes, 2003). One type of calcium channel, the transient (T)-type or low voltage-activated calcium channel, is implicated in the generation of normal brain rhythms, including the spindle waves recorded in the electroencephalogram (EEG) during sleep. T-type currents were first identified in thalamocortical circuitry by Jahnsen and Llinás (1984a,b) based on intracellular recordings in guinea-pig thalamic neurons. Similar recordings have since been made in other species, including current clamp recordings in monkey thalamic neurons (e.g. Crunelli et al., 1989; Coulter et al., 1989; Ramcharan et al., 2000; Monckton and McCormick, 2003). In all cases, inward T-type currents, activated at hyperpolarized membrane potentials, produce a depolarization that elicits high frequency bursts of action potentials. While these bursts participate in normal thalamic oscillations, they are also involved in several disorders of brain rhythms (Jeanmonod et al., 2001; Llinás et al., 2001; McCormick and Contreras, 2001).

Three structurally and functionally distinctive T-type calcium channels have been cloned, denoted voltage-dependent calcium channel (Ca_v)3.1, Ca_v3.2 and Ca_v3.3 (Perez-Reyes, 1999; Catterall et al., 2003). Electrophysiological recordings from cell lines engineered to express these different transcripts (and a number of splice variants) have revealed functional differences in the calcium currents carried by these channels (Klöckner et al., 1999). Moreover, *in situ* hybridization studies have revealed that these channels are differentially distributed throughout the brain (Talley et al., 1999). In the rat thalamus, Ca_v3.1 is found predominantly in relay neurons, and has an intriguing reciprocal relationship with thalamic reticular nucleus neurons, which weakly express Ca_v3.1 but strongly express Ca_v3.3. Findings such as these portray a functional diversity that may underlie differences in the tendency of neurons in different regions of the brain to burst, as well as provide a potential explanation for observed differences in the native currents found in different brain regions (Huguenard and Prince, 1992; Tarasenko et al., 1997; Joksovic et al., 2004).

Despite the clear importance of T-type channels to neuronal bursting and pacemaker activity in humans and their potential role in disorders of thalamic rhythms, there have been no direct recordings of the underlying native current under voltage clamp conditions in a non-human primate, and the expression patterns of T-type calcium channel transcripts in primate relay nuclei are unknown. We studied the characteristics of native T-type calcium

currents using whole cell recordings (either high impedance electrodes for current clamp measures or patch electrodes for voltage clamp) in brain slices of the dorsal lateral geniculate nucleus (LGN) of the cynomolgus macaque. Additionally, using reverse transcriptase PCR (RT-PCR) we identified the three major T-type calcium channel variants that contribute to native currents in the LGN of the macaque.

Our study shows that the key features of native T-type calcium currents and associated thalamocortical bursts are present in the primate brain and bear striking similarities with those recorded in other species. Knowledge of the details of these currents and the underlying channel distributions in primates will further illuminate the role of these channels in human health and disease.

EXPERIMENTAL PROCEDURES

These studies were carried out in conjunction with other studies using tissues recovered after necropsy. Cynomolgus macaques underwent necropsy in accord with protocols approved by the Wake Forest University Health Sciences Animal Care and Use Committee and in agreement with National Institutes of Health and U.S. Department of Agriculture Guidelines, including measures to eliminate suffering and to reduce animal numbers to a minimum. (Ariwodola et al., 2003). Animals were perfused through the heart with ice-cold artificial cerebrospinal fluid (ACSF) containing (in mM): 124 NaCl, 5 KCl, 2 MgSO₄, 2 CaCl₂, 23 NaHCO₃, 3 NaH₂PO₄, 10 glucose (pH 7.4, osmolarity 290–300 mOsm) oxygenated with 95% O₂:5% CO₂. All of the remaining brain tissue, as well peripheral tissues including the heart and liver, was used in other ongoing studies within the Center for the Neurobehavioral Study of Alcohol at Wake Forest University School of Medicine, or was stored at –80 °C for later use.

After necropsy a tissue block containing the LGN was immediately immersed in oxygenated (95% O₂:5% CO₂), ice cold sucrose-substituted ACSF containing (in mM): 220 sucrose, 12 MgSO₄, 10 glucose, 2 KCl, 1.5 NaH₂PO₄, 26 NaHCO₃, 0.2 CaCl₂ (pH 7.4, osmolarity 290–300 mOsm). A block of tissue containing the LGN was sectioned on a vibratome (model OTS 4000, Electron Microscopy Sciences, Fort Washington, PA, USA) at 400 μm, and slices were maintained in oxygenated, warm (34 °C) ACSF of the same composition as the perfusion ACSF, for at least 1.5 h before being transferred to a recording chamber (Harvard Apparatus, Holliston, MA, USA). Slices were recorded from using “blind” recording techniques, from 400 μm slices. For high impedance electrode recordings, slices were placed on a nylon mesh in a recording chamber at an interface of warmed (34 °C), oxygenated (95% O₂, 5% CO₂) air and buffer. For whole cell patch recordings, slices were submerged in oxygenated ACSF at 34 °C unless otherwise stated. Oxygenated ACSF was perfused at 2 ml per minute.

Recordings

Sharp electrodes (50–100 MΩ) were pulled from borosilicate glass (Sutter Instruments, Novato, CA, USA) with a P-87 horizontal puller (Sutter Instruments) and filled with 4 M potassium acetate. Patch pipettes (5–10 MΩ) were pulled from the same glass with a PC-10 vertical puller (Narishige International USA, Inc., East Meadow, NY, USA), and were filled with an internal solution containing (in mM): 100 gluconic acid, 100 CsOH, 10 NaCl, 10 HEPES, 20 TEA-Cl, 1 EGTA, 4 ATP (pH 7.3 with 2 N CsOH, osmolarity 270–290 mOsm). A liquid junction potential of +7 mV, determined experimentally, was corrected for post hoc. Cellular activity was acquired with an AxoClamp 2B amplifier (Axon Instru-

ments, Union City, CA, USA), digitized with a Digidata 1322 (Axon Instruments), and analyzed using pCLAMP 9.0 software (Axon Instruments). To acquire cells for voltage clamp, patch pipettes were advanced “blind” through tissue in bridge mode until encountering a cell, a >1 GΩ seal was formed, the membrane ruptured to allow whole cell access, and the amplifier was then switched to single-electrode voltage clamp recording mode. Current clamp recordings were included if the recording duration exceeded 10 min, with a resting membrane potential of –50 mV or less, and overshooting action potentials. For all voltage clamp experiments, tetrodotoxin (TTX, 1 μM; Alomone Laboratories, Jerusalem, Israel) was included in ACSF to block sodium action potentials.

Boltzmann analysis

Average peak inactivation currents were normalized to the peak of the maximally available current (I/I_{max}). This relative current was plotted as a function of pre-pulse potential and fitted with a Boltzmann equation: $I = I_{max}/(1 + \exp[(V - V_{1/2})/k])$ to derive, by least squares fits, the half-maximal voltage ($V_{1/2}$) and slope factor (k) values (Coulter et al., 1989; Crunelli et al., 1989).

Total RNA preparation

Total RNA was prepared from the thalamus (LGN, Magno and Parvo regions) of adult cynomolgus macaques using TriReagent (Molecular Research Center, Cincinnati, OH) according to the manufacturer’s protocol. RNA was further purified using Qiagen Mini Spin Columns (Valencia, CA) according to the manufacturer’s instructions. RNA concentrations were determined spectrophotometrically by measuring the absorption at 260 nm in a NanoDrop-1000 spectrophotometer (NanoDrop, Wilmington, DE). RNA quality was assessed by electrophoresis in 1% agarose formaldehyde gels (Ambion, Inc., Austin, TX).

Complementary DNA (cDNA) synthesis

cDNA was synthesized using the Invitrogen SuperScript III First Strand Synthesis System (Invitrogen Life Technologies, Carlsbad, CA, USA) for real-time PCR as per manufacturer’s instructions. Briefly, RNA was mixed with random hexamers (2.5 ng/μl final concentration) and dNTPs (0.5 mM final concentration) for 5 min at 65 °C and then placed on ice for at least 1 min. cDNA Synthesis Mix (Invitrogen Life Technologies) containing RT buffer, MgCl₂, DTT, RNaseOUT and SuperScript III RT (final concentrations 1×, 5 mM, 10 mM, 2 U/μl and 10 U/μl respectively) was then added at 25 °C for 10 min followed by cDNA synthesis at 50 °C for 50 min. cDNA reaction was terminated by incubation at 85 °C for 5 min. RNA was removed from RNA:DNA hybrids by incubation with RNase H at 37 °C for 20 min. cDNA was then diluted to a final concentration of 2 ng/μL.

Real-time RT-PCR

Real-time PCR was performed using the 5′-exonuclease method (Taqman) and an Opticon II system (MJ Research, Waltham, MA, USA). Taqman Universal PCR Master Mix (Applied Biosystems, Foster City, CA, USA) containing TaqDNA polymerase, dNTPs, (+dUTP), and buffers was used according to manufacturer’s instructions. Primer and probe combinations for each of the T-type calcium channel isoforms of the cynomolgus macaque were designed using Primer Express (Applied Biosystems). Probes were labeled 5′ with 6-FAM and 3′ with TAMRA or BHQ1 as quencher (Integrated DNA Technologies, Carolville, IA, USA). Sequences for each primer/probe were chosen from unique regions within each human gene by excluding conserved sequences. Regions surrounding known splice sites of the human subunits were also excluded. These sequences were cloned from cynomolgus macaque total RNA by RT-PCR and sequenced. For α1G (Ca_v 3.1:

GenBank # AY268438), the primer/probe set was GCCAGACCG-GAAGAATTTTG (5' primer), CCTGGGTGAGGATCTGAAAGAC (3' primer), and TCCTTGCTCTGGGCCATCGTCAC (probe). For $\alpha 1H$ (Ca, 3.2: GenBank # AY268439), the set was TGGTGGTG-GAGACGCTGAT (5' primer), GCAGCAGATGAGGACGATGTT (3' primer), and TCGTCACTCAGGCCATCGG (probe). Finally, for $\alpha 1I$ (Ca, 3.3: GenBank # AY268440), the set was CGCCCGTTGCCT-TCTTCT (5' primer), GCACACCATCTTGATACACCAGTT (3' primer), and TGCGACAGACCACCAGCCCC (probe).

RESULTS

Intracellular recordings were obtained from 72 LGN neurons from thalamic slices maintained *in vitro*. Of these, 52 neurons, with a mean resting membrane potential of -61.1 ± 1.6 mV, were recorded under current clamp conditions with high impedance electrodes, and 20 neurons, with a mean resting membrane potential of -62.3 ± 1.5 mV were recorded under voltage clamp conditions. All recordings were made from parvocellular laminae (layers 4–6) of the LGN.

Characteristics of bursts and underlying native T-type currents

The responses of LGN cells to depolarizing current pulses are shown in Fig. 1. During current clamp recordings, depolarizing LGN cells by injecting currents from holding potentials near -60 mV resulted in tonic streams of action potentials. While in some cells the frequency of tonic firing increased in proportion to the depolarizing step, in many

cases tonic firing was sporadic, with interruptions in the tonic firing sequences (Fig. 1A, second trace; $n=9$). A low threshold burst could be reliably elicited in response to depolarizing current pulses from a relatively hyperpolarized membrane potential (Fig. 1B). All cells tested with this protocol showed this bursting response pattern. Burst firing in monkey LGN cells, as in other species, was expressed as triangular waveform with a burst of two to seven fast action potentials (with interspike intervals of ~ 4 ms or less) occurring at the peak of the underlying Ca^{2+} mediated depolarization (Jahnsen and Llinás, 1984a,b; Lu et al., 1992; Monckton and McCormick, 2003; Ramcharan et al., 2000).

In order to study the current underlying monkey thalamic bursts, we used patch clamp techniques with TTX included in the ACSF to block voltage-dependent Na^+ currents. The voltage dependent inactivation of the T-type current is illustrated in Fig. 2. T-type current was inactivated through a series of depolarizing command potentials, progressing at 3 mV increments, starting at -132 mV, and stepping to -60 mV. Peak inactivation ($n=5$) current was normalized to the peak of maximally available current (I/I_{max}). The mean I_{max} elicited was 799 ± 142 pA. The mean \pm S.E.M. of I/I_{max} was plotted as a function of the prepulse command potential and fitted with a Boltzmann distribution as shown in Fig. 2B. Our results indicate the range of current inactivation was between -70 and -110 mV, the current inactivation k was 5.6, and the T-type

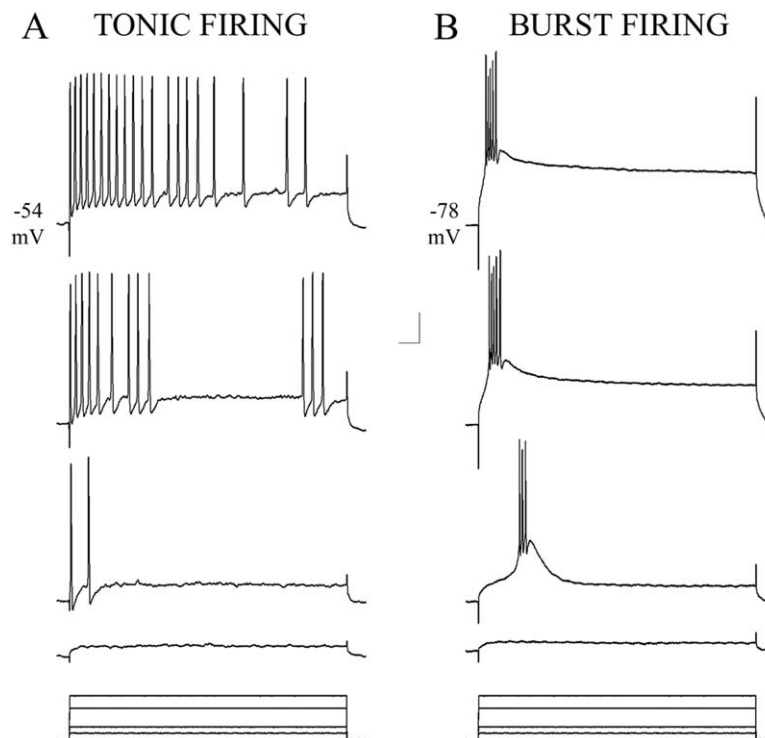


Fig. 1. Tonic and burst response modes of monkey thalamic neurons. (A) A series of depolarizing current steps (ranging from 0.1–0.7 nA) from a holding potential of -54 mV elicited an initial passive response followed by progressive regular spiking from LGN neurons. (B) The same series of depolarizing current steps from -78 mV elicited stereotypical burst responses composed of a triangular depolarization with three to five action potentials at the peak. Scale bar=20 mV, 40 ms.

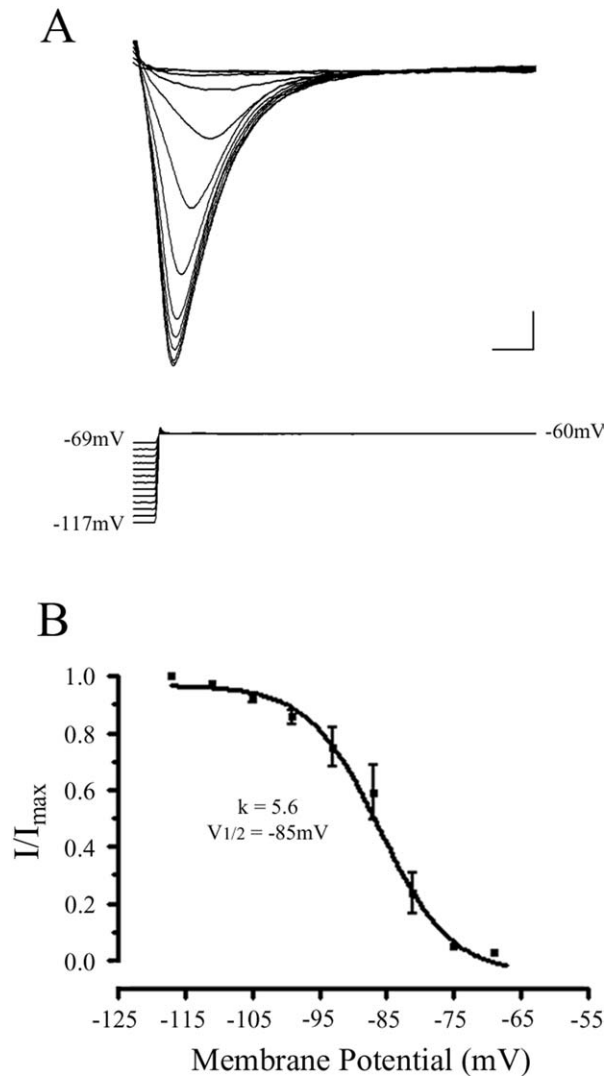


Fig. 2. Voltage dependent steady-state inactivation of T-type calcium current in LGN relay neurons. Inactivation kinetics were measured in response to a series of depolarizing command potentials from -132 mV to -63 mV, held for 1 s, then stepping to -60 mV, although the range of voltages producing inactivation, as shown, was between -117 mV to -69 mV. (A) Representative traces showing inactivation of T-type current using the command potentials shown below the set of traces. (B) Currents elicited at each command potential were normalized to the peak current elicited (I/I_{max}) and plotted against the command potential. The data were fit with a Boltzmann function ($n=5$). The k and $V_{1/2}$ derived from the Boltzmann are shown on the graph. Error bars represent standard error of the mean. Scale bar=100 pA, 30 ms.

current $V_{1/2}$ was -85 mV. These data for T-type current inactivation are in agreement with previous observations of native current studied *in vitro* in rodent and carnivore recorded under similar conditions (Coulter et al., 1989; Hernandez-Cruz and Pape, 1989; Mu et al., 2003).

Recovery from inactivation

Bursts can be elicited in LGN thalamocortical cells of other species by injecting hyperpolarizing current pulses into the cell, resulting in the deinactivation of the T-type current followed by activation that occurs during repolarization of

the membrane (Jahnsen and Llinás, 1984a,b; Kim et al., 1995; Bal et al., 1995a,b), a process that reflects recovery from channel inactivation.

We studied the time-dependent process of recovery from inactivation of native T-type current in 11 LGN cells with voltage clamp recordings (Fig. 3). Cells were hyperpolarized to -115 mV for 1300 ms then depolarized to -60 mV to completely inactivate the T-type current. The amplitude of the current elicited was used as I_{max} for comparisons to a test pulse of -60 mV after hyperpolarizations of varying time intervals (10–600 ms) to -115 mV. The amplitude of the current elicited from this test pulse was divided by I_{max} to characterize the time course of removal of inactivation. I_{max} for the population of cells was found to be 702 ± 71 pA. As shown in Fig. 3B, I/I_{max} was plotted against the time interval of hyperpolarization, and the data points were best fit with a single exponential decay function with a time constant of 49.4 ms (95% confidence interval=45.3–54.3 ms).

In current clamp recordings, monkey burst responses showed a characteristic refractory property consistent with removal of inactivation. As shown in Fig. 4A, this was observed as rebound responses that began as subthresh-

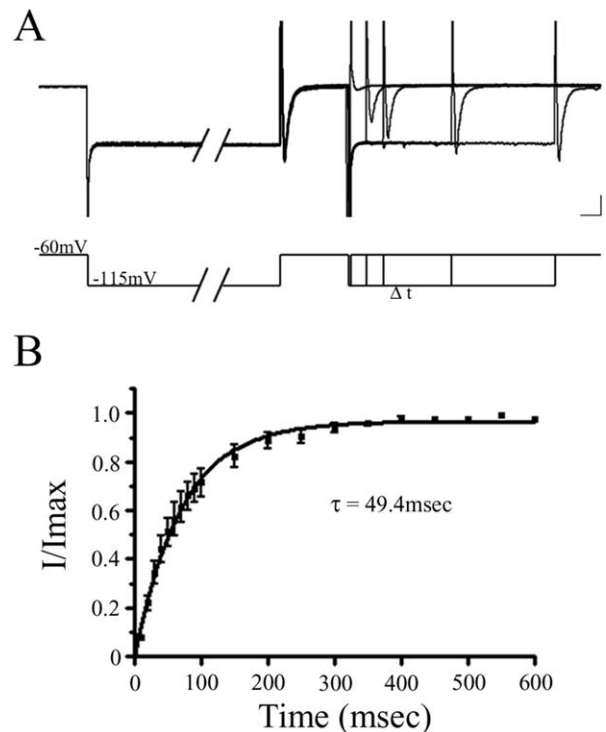


Fig. 3. Time dependence of recovery from inactivation in LGN relay neurons. (A) Representative voltage clamp traces illustrating time dependent process of recovery of T-type current following complete inactivation. Cells were hyperpolarized to -115 mV for 1300 ms then stepped to -60 mV to elicit a maximal T-type current. They were then stepped back to -115 mV for 10–600 ms and released again to -60 mV. The first current elicited in each sweep was deemed I_{max} , and the subsequently elicited current was divided by this to arrive at I/I_{max} which was plotted against the time of hyperpolarization (B). The data points were best fit with a single exponential decay function with a time constant of 49.4 ms ($n=11$). Error bars represent standard error of the mean. Scale bar=300 pA, 50 ms.

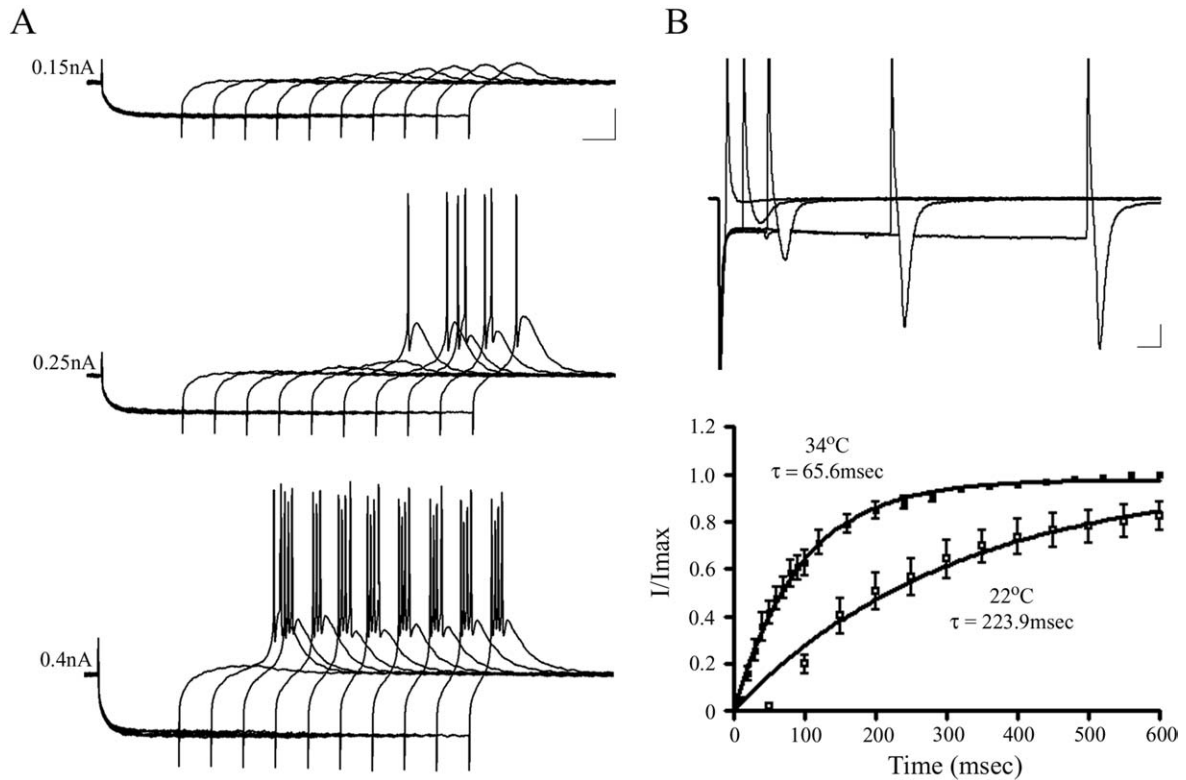


Fig. 4. Deactivation of bursts and T-type calcium current in LGN relay neurons. (A) Representative current clamp recordings illustrating time and hyperpolarization dependence of bursts. Cells were held at -60 mV and injected with the indicated current to hyperpolarize then for 150–600 ms, then released from hyperpolarization. With increased amplitude or duration of hyperpolarization, a greater low-threshold spike was elicited with more action potentials riding the crest. Scale bar=15 mV, 50 ms. (B) Representative voltage clamp traces illustrating the time dependence of T-type current recorded at 34°C . Cells were held at -60 mV, hyperpolarized to -110 mV for 10–600 ms then stepped back to -60 mV. The maximal current elicited was deemed I_{max} , and all current amplitudes were divided by this to give I/I_{max} which was plotted against the time of hyperpolarization. The data points were best fit with a single exponential decay function with a time constant of 65.6 ms ($n=4$). This protocol was also run in a separate group of cells recorded at room temperature (22°C). Under this temperature condition, peak current was not elicited until 900 ms of hyperpolarization, and these data points were best fit with a single exponential decay function with a time constant of 223.9 ms ($n=7$). Only those data points out to 600 ms are plotted on the graph. Error bars represent standard error of the mean. Scale bar=150 pA, 50 ms.

old low-threshold calcium depolarizations after short hyperpolarizing steps, which elicited bursts after sufficiently long periods of hyperpolarization. These responses were dependent both upon the amplitude of the hyperpolarization as well as the duration of the hyperpolarizing pulse. The responses were steeply graded in the numbers of spikes (one to five) that could be elicited in response to hyperpolarizing current injections ($n=10$).

Temperature affects the time-dependent kinetics of the removal of inactivation from T-type channels (Crunelli et al., 1989). We tested a group of cells at room temperature (22°C ; $n=7$) and a group at 34°C ($n=4$) to characterize deinactivation in LGN cells under both conditions, which are plotted in Fig. 4B. Peak current amplitudes were elicited by 450 ms hyperpolarization at 34°C while a hyperpolarization interval of 900 ms was required for peak current activation at 22°C . Current amplitudes were measured following varying lengths of hyperpolarizing steps between 10 and 1200 ms, and each current amplitude was divided by the peak current elicited to calculate an I/I_{max} value. These values were plotted against the hyperpolarizing interval and the data points were fit with single exponential functions with time constants of 223.9 ms (95%

confidence interval=197.2–258.9 ms) at 22°C and 65.6 ms (95% confidence interval=60.9–71.2 ms) at 34°C .

Voltage-dependent synaptic properties of monkey LGN neurons

A range of voltage-dependent responses of monkey LGN neurons recorded under current clamp conditions is illustrated in Fig. 5. Fig. 5A shows the firing pattern as well as synaptic responses over a range of membrane potentials. Hyperpolarizing current steps elicited bursts of action potentials upon repolarization of the membrane. Depolarizing current steps elicited tonic streams of action potentials, with the frequency of tonic spikes increasing in tandem with the size of the depolarizing current step ($n=6$). In the midpoint of the voltage step a 0.1 ms electrical stimulus was delivered through a bipolar stimulating electrode placed in the white matter adjacent to the LGN. In the presence of picrotoxin, a GABA_A receptor antagonist, excitatory postsynaptic potentials (EPSPs) could be elicited upon electrical stimulation (50–500 μA). The shape of these EPSPs varied with membrane potential. At -60

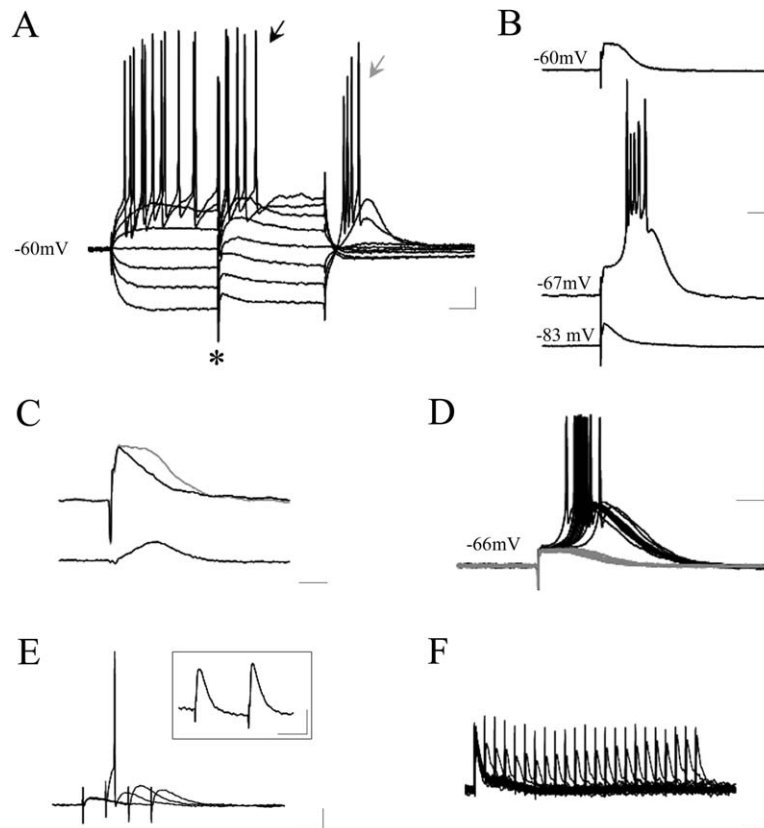


Fig. 5. Voltage dependent properties of monkey thalamic neurons. (A) Responses of an LGN neuron to a series of current pulses injected from -60 mV showing the voltage dependent responses of rebound bursts (gray arrow) in response to transient hyperpolarization and tonic streams of action potentials elicited by depolarizing current injections (black arrow). In the midpoint of the current step, a 0.1 ms electrical stimulus (asterisk) elicited an EPSP. Scale bar= 5 mV, 50 ms. (B) In the presence of picrotoxin, stimulation elicited a sharp, unimodal EPSP at -83 mV. At -67 mV, stimulation elicited a burst response, but at -60 mV the EPSP showed an additional late component. Scale bar= 10 mV, 20 ms. (C) Normalized and superimposed EPSPs for comparison of early and late EPSP components. The gray trace was recorded at -67 mV, and the black trace was recorded at -83 mV. The subtraction of the two traces, shown below, illustrates the time course of the late component. Scale bar= 10 ms. (D) The late component of the EPSP was capable of eliciting a burst of action potentials that arose from an underlying triangular depolarization. Fifty superimposed traces from EPSPs elicited from -66 mV show consistent latency of multimodal EPSPs, and variable latency of bursts responses arising from the EPSPs. Scale bar= 10 mV, 20 ms. (E) LGN cells display paired pulse facilitation in response to paired stimuli delivered at interstimulus intervals of 50 , 100 and 150 ms. At the shortest interval, a spike was elicited on the second stimulus. The inset trace illustrates another example of paired pulse facilitation in a different cell held at -72 mV. Of the 17 neurons in which paired-pulse EPSPs were recorded, three cells showed paired-pulse facilitation at a 100 ms interstimulus interval (ratio= 1.3 ± 0.1). Scale bars= 5 mV, 50 ms. (F) LGN cells also display paired pulse depression. The shortest interstimulus interval was 50 ms, and increased at 50 ms increments. At the shorter intervals, paired pulse depression was greatest, and with increased interstimulus intervals, the magnitude of depression was reduced. Of the 17 neurons in which paired-pulse EPSPs were recorded, 14 cells showed paired-pulse depression at a 100 ms interstimulus interval (ratio= 0.72 ± 0.04). Scale bar= 2 mV, 100 ms.

mV, the EPSPs appeared multimodal, consistent with *N*-methyl-D-aspartate (NMDA) and non-NMDA receptor contributions. At -67 mV, stimulation elicited a mixed response composed of an early EPSP followed by an occasional burst as reported in other species (Turner et al., 1994; Bartlett and Smith, 1999). At -83 mV, stimulation produced a sharper unimodal EPSP ($n=7$) (Fig. 5B). We compared normalized EPSPs at -83 mV and -67 mV (Fig. 5C). Subtraction of these traces indicates a late component in the EPSP recorded at -67 mV. Under our recording conditions, in which picrotoxin was included in the ACSF, EPSPs possessing this late component could elicit burst responses in LGN cells (Fig. 5D).

We also recorded pairs of EPSPs to determine whether they showed short term plasticity. Paired pulses have been shown to promote synaptic depression at retino-

geniculate synapses and facilitation at corticogeniculate synapses (Turner and Salt, 1998; Granseth et al., 2002; Alexander and Godwin, 2005). While determining the pathways of origin of these EPSPs was not possible, EPSPs in the monkey LGN showed both facilitation and depression (Fig. 5E–F).

Molecular characterization of T-type calcium channels in the LGN

Talley et al. (1999) reported the distribution of mRNA encoding the three known T-type channel transcripts in the rat brain. They reported greater expression of $\alpha 1G$ ($Ca_v3.1$) in thalamic relay nuclei, with little or no expression of $\alpha 1H$ ($Ca_v3.2$) and $\alpha 1I$ ($Ca_v3.3$). Using RT-PCR methods we examined the possible T-type channel tran-

scripts that may contribute to our electrophysiological observations. The LGN tissue used for molecular analyses was isolated from the face of fresh tissue blocks from four cases in which *in vitro* slices were prepared. In two additional cases, layers 5 and 6 (representing parvocellular layers), and layers 1 and 2 (representing magnocellular layers) were dissected from the tissue block.

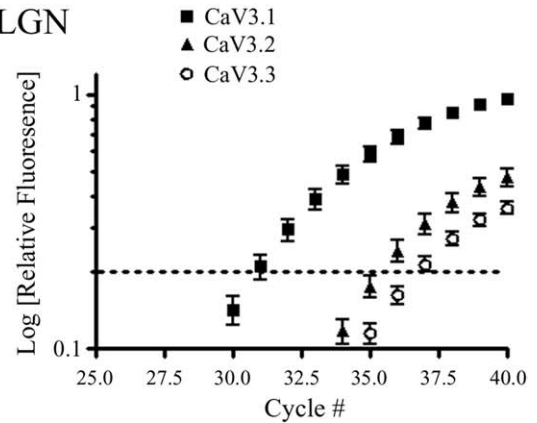
Fig. 6 shows relative gene expression profiles of the T-type channel transcripts. Of these, $Ca_v3.1$ expression was greater than both $Ca_v3.2$ and $Ca_v3.3$ in all examined tissues. $Ca_v3.1$ crossed the threshold cycle (C_T) around cycle number 31 in the LGN samples and at about cycle number 30 for both magnocellular and parvocellular subdivisions. $Ca_v3.2$ and $Ca_v3.3$ were expressed at approximately the same rate and crossed the threshold approximately five to six cycles later than $Ca_v3.1$. The relationship between the log[nanograms of total thalamic RNA] put into the PCR reaction and the relative expression level, represented by the C_T , of each gene product was linear over a wide range of concentrations (data not shown), indicating that C_T could be directly related to the amount of mRNA in the original sample. Thus, we conclude that $Ca_v3.1$ RNA is expressed in relatively higher abundance than both $Ca_v3.2$ and $Ca_v3.3$ in the LGN. The same pattern of gene expression for T-type calcium channels was observed in dissected whole LGN tissues, as well as parvocellular and magnocellular subdivisions of the LGN, showing that the molecular basis of burst firing does not differ between parallel visual processing streams.

DISCUSSION

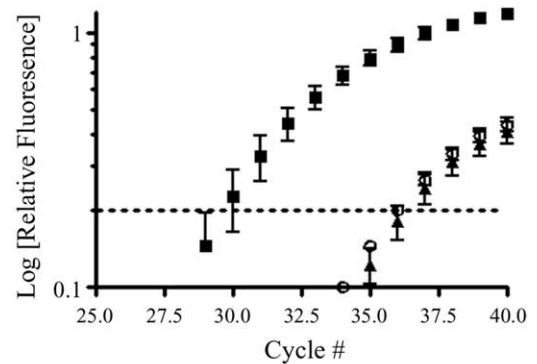
This study describes burst responses and the underlying native T-type calcium current in the cynomolgus macaque. We have found that LGN neurons display both burst and tonic modes of firing, with burst firing mode elicited by activation of the T-type calcium current. We have characterized the voltage-dependent process of T-type channel inactivation, as well as the voltage- and time-dependent process of recovery from inactivation (“deinactivation”). We have shown that “rebound” burst responses may be elicited through membrane repolarization and bursts may also be synaptically activated, arising from the late component of the EPSP. Finally, we have characterized and determined relative expression levels of the three known isoforms of the T-type calcium channel in the LGN.

This T-type current shows impressive similarity in basic voltage dependent properties, including inactivation and recovery from inactivation, with T-type current recorded from other species and from cloned human channels expressed in culture systems (Huguenard, 1996; Perez-Reyes, 2003). The T-type current inactivation kinetics determined through the Boltzmann analysis were consistent with previous reports with similar recording situations (Coulter et al., 1989; Crunelli et al., 1989; Mu et al., 2003). The current expressed a time-dependent recovery from inactivation (“deinactivation”) that has been shown to promote rebound bursts in response to strong hyperpolarizations such as GABAergic

A. LGN



B. Magno



C. Parvo

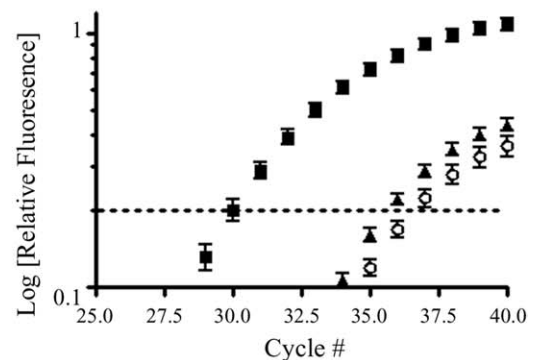


Fig. 6. T-type calcium channel gene expression in the LGN. Real-time RT-PCR was used to measure relative gene expression of $Ca_v3.1$, $Ca_v3.2$ and $Ca_v3.3$ in the monkey LGN. Gene expression for each T-type channel isoform is shown for tissue samples containing whole LGN (A) and samples from separate animals that represent the magnocellular (B) and parvocellular (C) subdivisions of the LGN, using primer/probe combinations specific for each isoform. Arbitrary assignment of a “cutoff” fluorescence level (dashed line) during the log linear portion of the fluorescence versus cycle relationship yields a “threshold” cycle that is directly related to the amount of cDNA present in the original sample. Data are represented as the mean \pm standard error of the mean, $n=4$.

inhibitory postsynaptic potentials (IPSPs). This refractory property factors prominently in the generation of spindle waves, which humans share with other mammals, and in hypersynchronous thalamic oscillations as

sociated with a number of disorders of thalamic rhythm (Jeanmonod et al., 2001; Llinás et al., 2001; McCormick and Contreras, 2001).

Burst responses have been observed in response to synaptically evoked IPSPs and EPSPs in a number of species (Scharfman et al., 1990; Turner et al., 1994; Bartlett and Smith, 1999), and we also observed bursts arising from EPSPs elicited by electrical stimulation of monkey LGN slices. While the origin of EPSPs recorded from monkey LGN cells could not be unequivocally identified, they show similarities in key properties to EPSPs recorded in other species, including a voltage dependency and multimodal appearance at depolarized membrane potentials. Synaptically elicited bursts arose from the late component of the EPSP, consistent with the NMDA component (Scharfman et al., 1990; Turner et al., 1994; Bartlett and Smith, 1999).

Using RT-PCR techniques in tissues from which our recordings were derived, we found that all three T-type calcium channels were expressed in the monkey LGN, though not in equal measure. We determined that the $Ca_v3.1$ transcript occurred in greater relative abundance than the $Ca_v3.2$ and $Ca_v3.3$ transcripts. This is consistent with *in situ* hybridization studies in rat which showed higher expression levels of $\alpha 1G$ ($Ca_v3.1$) in LGN, with other transcripts at levels of expression that were either below or near the threshold for detection (Talley et al., 1999).

Several studies have suggested that thalamic bursts may participate in relaying certain types of visual information to cortex (Guido et al., 1995; Reinagel et al., 1999), and that these bursts may occur in awake, behaving animals (Martinez-Conde et al., 2002; Ramcharan et al., 2001; Ruiz et al., 2006; Swadlow and Gusev, 2001; Weyand et al., 2001). The monkey LGN comprises six principal layers of neurons that represent the contralateral visual field. In addition to intrinsic GABAergic interneurons, three populations of relay neurons with physiologically distinct properties are found in the primate LGN. These include so-called magnocellular, parvocellular, and koniocellular types. Magnocellular neurons are sensitive to motion, are found in layers 1 and 2, and receive retinal input from parasol retinal ganglion cells (Schiller and Malpeli, 1978). Parvocellular neurons are sensitive to higher spatial frequency information, reside in layers 3 through 6, and receive excitatory retinal input from midget ganglion cells (Perry et al., 1984). Koniocellular neurons are interspersed within and between principal layers (though distinct laminae in the macaque are difficult to demonstrate), and receive input predominantly from blue-ON retinal ganglion cells (Martin et al., 1997). Because of these important functional differences between LGN cell types, and because bursts have been recorded in magnocellular and parvocellular neurons (Ramcharan et al., 2001; Ruiz et al., 2006) we also examined T-type channel gene expression for tissues dissected from layers 5 and 6, corresponding to the parvocellular subdivision of the LGN, and layers 1 and 2, corresponding to the magnocellular subdivision. We measured gene expression of T-type channels in both subdivisions, and found expression of all transcripts. We

found no evidence based on these samples that the relative level of expression of the three channels differed between magnocellular and parvocellular subdivisions. This suggests that whatever the roles burst responses play in thalamic rhythms or in visual processing, the biological basis for bursts is common to the different visual processing streams.

CONCLUSION

We have characterized the key properties of native T-type calcium currents in the cynomolgus macaque using a range of technical approaches. We have successfully implemented whole cell, voltage clamp recordings in adult monkey thalamus in order to directly record native T-type calcium currents. While such recordings in mature animals present a special challenge, and the numbers of observations are necessarily limited, they contribute an important translational linkage between burst responses and the underlying T-type currents performed in other species and the situation in humans. Current and voltage clamp recordings revealed that the key features of native T-type currents of the monkey are consistent with those recorded from other species. In addition, we showed that excitatory synaptic inputs to the monkey thalamus are capable of activating T-type burst responses. The physiological expression of neuronal T-type calcium channels is synonymous with burst firing in a variety of brain regions. Using RT-PCR we found that the molecular basis of these currents may depend more upon expression of the $Ca_v3.1$ transcript, which was expressed in higher relative abundance in the entire LGN as well as the important parvocellular and magnocellular subdivisions. The organization of the monkey LGN is homologous to that of humans, thus the results of our study should add to the framework for understanding the contribution of T-type calcium currents to thalamic bursts in humans. This is of particular importance because of the participation of bursts in a range of disorders of thalamic rhythm.

Acknowledgments—This work was supported by EY11695; AA013246; AA014063; AA11997; NS046222; Center for the Neurobehavioral Study of Alcohol.

REFERENCES

- Alexander GM, Godwin DW (2005) Presynaptic inhibition of corticothalamic feedback by metabotropic glutamate receptors. *J Neurophysiol* 94:163–175.
- Ariwodola OJ, Crowder TL, Grant KA, Daunais JB, Friedman DP, Weiner JL (2003) Ethanol modulation of excitatory and inhibitory synaptic transmission in rat and monkey dentate granule neurons. *Alcohol Clin Exp Res* 27:1632–1639.
- Bal T, von Krosigk M, McCormick DA (1995a) Role of the ferret perigeniculate nucleus in the generation of synchronized oscillations in vitro. *J Physiol* 483:665–685.
- Bal T, von Krosigk M, McCormick DA (1995b) Synaptic and membrane mechanisms underlying synchronized oscillations in the ferret lateral geniculate nucleus in vitro. *J Physiol* 483:641–663.
- Bartlett EL, Smith PH (1999) Anatomic, intrinsic, and synaptic properties of dorsal and ventral division neurons on rat medial geniculate body. *J Neurophysiol* 81:1999–2016.

- Catterall WA, Striessnig J, Snutch TP, Perez-Reyes E (2003) International Union of Pharmacology. XL. Compendium of voltage-gated ion channels: calcium channels. *Pharmacol Rev* 55:579–581.
- Coulter DA, Huguenard JR, Prince DA (1989) Calcium currents in rat thalamocortical relay neurones: kinetic properties of the transient, low-threshold current. *J Physiol* 414:587–604.
- Crunelli V, Lightowler S, Pollard CE (1989) A T-type Ca^{2+} current underlies low-threshold Ca^{2+} potentials in cells of the cat and rat lateral geniculate nucleus. *J Physiol* 413:543–561.
- Granseth B, Ahlstrand E, Lindstrom S (2002) Paired pulse facilitation of corticogeniculate EPSCs in the dorsal lateral geniculate nucleus of the rat investigated in vitro. *J Physiol* 544:477–486.
- Guido W, Lu SM, Vaughan JW, Godwin DW, Sherman SM (1995) Receiver operating characteristic (ROC) analysis of neurons in the cat's lateral geniculate nucleus during tonic and burst response mode. *Vis Neurosci* 12:723–741.
- Hernandez-Cruz A, Pape HC (1989) Identification of two calcium currents in acutely dissociated neurons from the rat lateral geniculate nucleus. *J Neurophysiol* 61:1270–1283.
- Huguenard JR (1996) Low-threshold calcium currents in central nervous system neurons. *Annu Rev Physiol* 58:329–348.
- Huguenard JR, Prince DA (1992) A novel T-type current underlies prolonged Ca^{2+} -dependent burst firing in GABAergic neurons of rat thalamic reticular nucleus. *J Neurosci* 12:3804–3817.
- Jahnsen H, Llinás R (1984a) Ionic basis for the electro-responsiveness and oscillatory properties of guinea-pig thalamic neurones in vitro. *J Physiol* 349:227–427.
- Jahnsen H, Llinás R (1984b) Electrophysiological properties of guinea-pig thalamic neurones: an in vitro study. *J Physiol* 349:205–226.
- Jeanmonod D, Magnin M, Morel A, Seigemund M, Cancro A, Lanz M, Llinás R, Ribary U, Kronberg E, Schulman J, Zonenshayn M (2001) Thalamocortical dysrhythmia. II. Clinical and surgical aspects. *Thalamus Relat Syst* 1:245–254.
- Joksovic PM, Brimelow BC, Murbartian J, Perez-Reyes E, Todorovic SM (2004) Contrasting anesthetic sensitivities of T-type Ca^{2+} channels of reticular thalamic neurons and recombinant Cav3.3 channels. *Br J Pharmacol* 144:59–70.
- Kim U, Bal T, McCormick DA (1995) Spindle waves are propagating synchronized oscillations in the ferret LGNd in vitro. *J Neurophysiol* 74:1301–1323.
- Klöckner U, Lee JH, Cribbs LL, Daud A, Hescheler J, Pereverzev A, Perez-Reyes E, Schneider T (1999) Comparison of the Ca^{2+} currents induced by expression of three cloned α 1 subunits, α 1G, α 1H and α 1I, of low-voltage-activated T-type Ca^{2+} channels. *Eur J Neurosci* 11:4171–4178.
- Llinás R, Ribary U, Jeanmonod D, Cancro R, Kronberg E, Schulman J, Zonenshayn M, Magnin M, Morel A, Siegmund M (2001) Thalamocortical dysrhythmia I. Functional and imaging aspects. *Thalamus Relat Syst* 1:237–244.
- Lu SM, Guido W, Sherman SM (1992) Effects of membrane voltage on receptive field properties of lateral geniculate neurons in the cat: contributions of the low-threshold Ca^{2+} conductance. *J Neurophysiol* 68:2185–2198.
- Martin PR, White AJ, Goodchild AK, Wilder HD, Sefton AE (1997) Evidence that blue-on cells are part of the third geniculocortical pathway in primates. *Eur J Neurosci* 9:1536–1541.
- Martinez-Conde S, Macknik SL, Hubel DH (2002) The function of bursts of spikes during visual fixation in the awake primate lateral geniculate nucleus and primary visual cortex. *Proc Natl Acad Sci U S A* 99:13920–13925.
- McCormick DA, Contreras D (2001) On the cellular and network bases of epileptic seizures. *Annu Rev Physiol* 63:815–846.
- Monckton JE, McCormick DA (2003) Comparative physiological and serotonergic properties of pulvinar neurons in the monkey, cat and ferret. *Thalamus Relat Syst* 2:239–252.
- Mu J, Carden WB, Kurukulasuriya NC, Alexander GM, Godwin DW (2003) Ethanol influences on native T-type calcium current in thalamic sleep circuitry. *J Pharmacol Exp Ther* 307:197–204.
- Perez-Reyes E (1999) Three for T: molecular analysis of the low voltage-activated calcium channel family. *Cell Mol Life Sci* 56:660–669.
- Perez-Reyes E (2003) Molecular physiology of low-voltage-activated t-type calcium channels. *Physiol Rev* 83:117–161.
- Perry VH, Oehler R, Cowey A (1984) Retinal ganglion cells that project to the dorsal lateral geniculate nucleus in the macaque monkey. *Neuroscience* 12:1101–1123.
- Ramcharan EJ, Cox CL, Zhan XJ, Sherman SM, Gnadt JW (2000) Cellular mechanisms underlying activity patterns in the monkey thalamus during visual behavior. *J Neurophysiol* 84:1982–1987.
- Ramcharan EJ, Gnadt JW, Sherman SM (2001) The effects of saccadic eye movements on the activity of geniculate relay neurons in the monkey. *Vis Neurosci* 18:253–258.
- Reinagel P, Godwin D, Sherman SM, Koch C (1999) Encoding of visual information by LGN bursts. *J Neurophysiol* 81:2558–2569.
- Ruiz O, Royal DW, Sary G, Chen X, Schall JD, Casagrande VA (2006) Low-threshold Ca^{2+} -associated bursts are rare events in the LGN of the awake behaving monkey. *J Neurophysiol*. Epub ahead of print.
- Schiller PH, Malpeli JG (1978) Functional specificity of lateral geniculate nucleus laminae of the rhesus monkey. *J Neurophysiol* 41:788–797.
- Scharfman HE, Lu SM, Guido W, Adams PR, Sherman SM (1990) N-methyl-D-aspartate receptors contribute to excitatory postsynaptic potentials of cat lateral geniculate neurons recorded in thalamic slices. *Proc Natl Acad Sci U S A* 87:4548–4552.
- Swadlow HA, Gusev AG (2001) The impact of “bursting” thalamic impulses at a neocortical synapse. *Nat Neurosci* 4:402–408.
- Talley EM, Cribbs LL, Lee JH, Daud A, Perez-Reyes E, Bayliss DA (1999) Differential distribution of three members of a gene family encoding low voltage-activated (T-type) calcium channels. *J Neurosci* 19:1895–1911.
- Tarasenko AN, Kostyuk PG, Eremin AV, Isaev DS (1997) Two types of low-voltage-activated Ca^{2+} channels in neurons of rat laterodorsal thalamic nucleus. *J Physiol* 499:77–86.
- Turner JP, Leresche N, Guyon A, Soltesz I, Crunelli V (1994) Sensory input and burst firing output of rat and cat thalamocortical cells: the role of NMDA and non-NMDA receptors. *J Physiol* 480:281–295.
- Turner JP, Salt TE (1998) Characterization of sensory and corticothalamic excitatory inputs to rat thalamocortical neurones in vitro. *J Physiol* 510:829–843.
- Weyand TG, Boudreaux M, Guido W (2001) Burst and tonic response modes in thalamic neurons during sleep and wakefulness. *J Neurophysiol* 85:1107–1118.